ISSN 0354-8724 (hard copy) | ISSN 1820-7138 (online)

Effective Street Geometry and Shading Strategies for Pedestrian Thermal Comfort: A Scenario Based Simulation Approach

Shivanjali Mohite[A1]

Received November 20, 2025| Revised: January 10, 2026| Accepted: January 13, 2026

doi: 10.5937/gp29-62910

Abstract

The development of urban heat issues poses significant challenges for pedestrians in tropical cities, necessitating climate-responsive street design. This study employs a scenario-based simulation approach to determine optimal combinations of street geometry and shading strategies that enhance Pedestrian Thermal Comfort (PTC). Using ENVI-met, this study simulated 90 scenarios by combining geometric variables, such as aspect ratio (AR), building typology (BT), and street orientation, with five shading strategies in Nagpur City, India. The modified Physiological Equivalent Temperature (mPET) index was calculated for each scenario using a pre-trained machine learning model. Results quantified that canopy shading was the most effective strategy, reducing mPET by up to 7°C in E-W streets. The effective street geometric combination was a N-S oriented street with a deep AR and linear BT, which consistently achieved the lowest mPET values (33.1–35.8°C). The study concludes with a rating matrix that guides the integration of shading design with street geometry to achieve thermally resilient streets.

Keywords: Pedestrian Thermal Comfort; Urban Street Geometry; ENVI-met; Machine Learning; Microclimate

Introduction

Urban areas worldwide are experiencing profound transformations in their thermal environments, driven by the dual forces of climate change and rapid urbanization. The Intergovernmental Panel on Climate Change (IPCC) has emphasized the increase in vulnerability of tropical and subtropical regions to the impacts of climate change, projecting a scenario where these areas face notable seasonal and annual temperature variations compared to mid-latitudes (IPCC, 2022). This susceptibility arises from the narrow environmental tolerances inherent to tropical ecosystems (Marcotullio et al., 2021). Within these regions, the indicator of climate change is increasingly evident through the intensification of the Urban Heat Islands (UHI) effect, where urban areas are significantly warmer than surrounding rural areas and the frequency of heat waves (Harrington et al., 2016; Russo et al., 2019).

The UHI effect and intensifying heat waves can exacerbate thermal stress, which not only causes significant thermal discomfort but also alters the patterns of outdoor physical and social activities in urban public spaces (Dunjić, 2019; Kim & Brown, 2021; Kotharkar et al., 2019). For pedestrians, excessive heat stress has been reported as a critical barrier to walking activity, which, in turn, can deteriorate walkability, street liv-

1 Corresponding author: Shivanjali Mohite; e-mail: shivanjali.mohite@students.vnit.ac.in
A Visvesvaraya National Institute of Technology, Nagpur, India; ORCID: 0009-0009-8349-3982

ability, and urban vitality (Paul et al., 2025; Tumini et al., 2016). Improving Pedestrian Thermal Comfort (PTC), which is defined as the microclimatic state in which individuals can walk the maximum distance without discomfort or being compelled to modify their environment (Vasilikou & Nikolopoulou, 2020), is therefore essential for urban planning and design.

PTC is governed by a complex interaction between meteorological factors, such as air temperature (Ta), relative humidity (RH), solar radiation (SR), and wind speed and street geometry (Aghamolaei et al., 2023; Khaire et al., 2024; Zhao et al., 2024). Key geometric parameters, including the aspect ratio (AR), street orientation, and the Sky View Factor (SVF), regulate the microclimate within urban canyons by controlling solar access and wind flow (Achour-Younsi & Kharrat, 2016a; Albdour & Baranyai, 2019; Porwal et al., 2025).

Among these variables, solar radiation has the most significant impact on outdoor human thermal sensation (Arif & Yola, 2020; Lin, 2009; Yilmaz et al., 2023). To mitigate discomfort from direct solar exposure, pedestrians consistently exhibit a preference for moving into shaded areas (Hess et al., 2023; Jamei & Rajagopalan, 2017; Watanabe & Ishii, 2016). Thus, effective shading is a fundamental requirement for sustaining long-term outdoor thermal comfort (Lin et al., 2010). The shaded pedestrian environments attract people and encourage walking, yielding direct co-benefits for public health, local economies, and environmental sustainability (Kim & Brown, 2021). The primary mechanism of shading is the reduction of the Mean Radiant Temperature (Tmrt), which represents the sum of all shortwave and longwave radiation in the pedestrian environment. Effective shading not only blocks direct sunlight but also keeps adjacent urban surfaces cooler, which in turn reduces local air temperatures.

Numerous studies have emphasized the significance of shading. For instance, a study conducted in the hot-arid climate of Cairo found that shading can improve thermal comfort by up to 2.3°C on the PET index scale (Elrefai & Nikolopoulou, 2023). Similarly, in Cordoba, Spain, shading interventions achieved up to a 16°C reduction in ground surface temperatures and up to a 6°C reduction on building façades during peak summer (Srivanit & Jareemit, 2019). Field surveys in Arizona also observed the positive impact of shading on enhancing PTC, with no reported difference in perceived comfort due to the type of shade (tree or solar canopy) in the hot-dry climate (Dzyuban et al., 2022). Urban shading can be achieved through a combination of factors, including geometric configurations such as aspect ratio and orientation, vegetative shading through street trees and green corridors, and artificial systems such as arcades, canopies, and other shading structures (Li et al., 2023; Siqi et al., 2023).

Though the efficiency of shading is well documented along with the ways to achieve it, designing thermally comfortable street spaces remains an adaptive challenge in urban design and microclimate studies. Building upon the previous part of this study on PTC, which established thermal comfort thresholds (Mohite & Surawar, 2024a) and utilized machine learning for evaluation of the thermal comfort index - modified Physiological Equivalent Temperature (mPET) (Mohite & Surawar, 2024b). This study aims to assess street geometry and shading strategies to determine configurations that provide the highest thermal benefits. The following background study examines the roles of street geometry and vegetation in shaping the urban microclimate.

Background Study

Impact of street geometry on microclimate and pedestrian thermal comfort

Street geometry is mainly quantified through parameters such as sky view factor (SVF), aspect ratio (AR), street orientation, building typology, and vegetation, etc. (Achour-Younsi & Kharrat, 2016b; Albdour & Baranyai, 2019). These parameters regulate the degree of street shading and influence microclimate conditions, particularly mean radiant temperature (Tmrt), surface temperature, and airflow patterns (Aicha et al., 2022; Bourbia & Awbi, 2004). The studies on PTC in urban canyons are categorized into two categories. The first category focuses on urban geometry parameters such as AR and street orientation and aims to optimize different building heights with orientation to determine which urban geometry combination reduces thermal stress (Chen et al., 2012; Y. Zhang et al., 2017). The second type of study focuses on optimizing thermal comfort using different types of vegetation, their placement, and other factors (Sayad et al., 2021; Segura et al., 2022).

Street geometry plays an important role in controlling the amount of solar radiation received and reradiated by urban structures. In an urban canyon, the surface temperatures of nearby buildings and the heat they transfer to the air significantly affect the air temperature (Ta). This influence is largely determined by the presence or absence of direct solar exposure.

Sky View Factor

Sky View Factors (SVF) indicate the proportion of the visible sky at a particular location. It is a ratio of the radiation received at a given point to the overall radiation in the hemispheric area surrounding that point (Johnson & Watson, 1984). This ratio ranges from 0 to 1, where 0 indicates a completely obstructed sky, and 1 denotes a completely clear sky. The SVF is crucial in influencing PTC in urban environments. Studies have shown that modifications in SVF can significantly impact outdoor thermal comfort (Arif & Yola, 2022; Ratnayake et al., 2022). Higher SVF values, indicating a more visible sky area, are associated with a high thermal comfort index value and vice versa (Aicha et al., 2022). SVF modifications through urban vegetation, such as street trees, have been identified as effective strategies to enhance PTC, especially in warm and humid climates (Ratnayake et al., 2022). Additionally, SVF is significantly correlated with thermal comfort parameters like Tmrt, emphasizing its importance in creating comfortable outdoor spaces for pedestrians. In a study in the warm and humid context of Colombo, Sri Lanka, the correlation between the SVF modifications and outdoor thermal comfort was analyzed in the context of street tree planting, and it was identified that trees modifying SVF enhance daytime thermal comfort for pedestrians significantly (Ratnayake et al., 2022). Similarly, in a study in the tropical climate of Singapore and India, SVF was identified as a major factor influencing thermal comfort, particularly on E-W-oriented streets (Xu et al., 2023).

Street orientation and Aspect Ratio

Aspect ratio (AR) is the ratio between the canyon walls' average height (H) and width (W). Studies have shown that the AR and orientation of streets significantly impact thermal comfort in urban environments (Chatzidimitriou & Yannas, 2017; Lobaccaro et al., 2019). Abdollahzadeh & Biloria (2021) found that among four design factors, street orientation is the most influential (46.42%), followed by AR (30.59%). According to Sharmin & Steemers (2013) N–S streets have a lower Tmrt than E–W streets, and the thermal comfort index physiological equivalent temperature (PET) is mostly influenced by shade availability. Srivanit & Jareemit (2019) observed that an N–S-oriented canyon has the lowest Tmrt, followed by NW–SE- and NE–SW-oriented canyons, and the worst situation is in the E–W canyon. Raising H/W also considerably reduces Tmrt in all canyon orientations except E–W. Also, Achour-Younsi & Kharrat (2016a) found that the N–S streets with the highest AR ratio have the most comfortable values, and those with E–W orientation are the least pleasant. In Egypt, an AR of 2.5 was found to provide the best thermal conditions in both Alexandria and Aswan (Abdelhafez et al., 2022). In a study in Malaysia, it was observed that asymmetrical streets with an AR of 0.8–2 reduce morning microclimate and night heat islands, and an AR of 2-0.8 reduces surface temperature by 10-14°C (Qaid & Ossen, 2015). Similarly, a study in Kolkata, India, observed that the AR of 2.5 reduces the thermal comfort index value (PET) by 5-9°C, and the orientation angle of 30-60° with wind direction improves the microclimate (De & Mukherjee, 2018). Furthermore, studies in Saudi Arabia emphasized the importance of multi-asymmetrical aspect ratios in improving urban pedestrian microclimates, with a gradual increase in ARs leading to reduced air temperatures and increased wind velocities (Abdelhafez et al., 2022).

Building typology

The building typology (BT) refers to how compactly the buildings are placed along the street; thus, it is categorized as linear, where there is no gap between adjacent buildings; singular, where there are appropriate setbacks between buildings; and scattered, where the buildings are placed far from each other. It governs microclimate by solar permeability, heat-trapping, and wind flow throughout the length of a street (Albdour & Baranyai, 2019). Zhang et al. (2022) indicated that the microclimate clearly differed with variations in building arrangement and enclosure. The building typology for each side of the street is determined using the Building Surface Area Fraction (BSF). BSF is a portion of the sidewalk with a building adjacent to it (Kotharkar et al., 2023).

$$\mathrm{BSF} = \frac{\text{Length of total building surface facing the street}}{\text{Total length of sidewalk}}$$

(Equation 1)

Impact of shading intervention on microclimate and pedestrian thermal comfort

Vegetation

Vegetation, primarily trees helps to cool the surrounding air as their canopy blocks radiation and evapotranspiration, where the water released from leaves absorbs heat from air (Armson et al., 2012; Konarska et al., 2016). Trees alter the microclimate by changing the amount of solar and terrestrial radiation received on the ground through shading (Speak et al., 2020). Most of these studies reported that the cooling capacity of the trees depends mainly on the canopy

coverage and planting density, etc. (Raman et al., 2021). A study in the tropical city of Bangalore, India, showed that street segments with trees recorded lower ambient air temperature by 5.6 °C on average (Vailshery et al., 2013). Field measurements in the hot-humid climate of Singapore showed a temperature difference of 1.5–2.8 °C between tree canopies and surrounding areas (Lindberg & Grimmond, 2011). Similarly, a study in Roorkee highlights the role of green-blue infrastructure, particularly the combination of low sky-view factor (SVF), dense canopy trees, and proximity to water, in reducing heat stress (Manavvi & Milosevic, 2025).

Artificial Shading Structures

Artificial shading is created by permanent built structures such as arcades, awnings, and pedestrian canopies. This approach offers a controllable solution that can be precisely designed to match specific street geometry. Its cooling mechanism relies solely on blocking solar radiation; unlike vegetation, it does not provide additional cooling through evapotranspiration. In Cairo, overhead shading improved thermal comfort by up to 2.3°C on the PET scale (Galal et al., 2020). Field studies in Arizona reported that pedestrian comfort under canopies was perceived to be equal to comfort under tree shade, highlighting that blocking radiation is the primary factor (Middel et al., 2016).

Therefore, achieving optimal PTC requires the strategic integration of shading design with urban geometry. While prior research mentioned above has established the importance of individual parameters, their synergistic combination through specific shading strategies is critical. This study addresses this necessity by evaluating the effectiveness of various shading strategies across different street geometric combinations.

Methodology

This study aims to determine street geometry and shading strategies to identify configurations that provide the highest thermal benefits in an urban street on hot summer days through ENVI-met simulation. The methodology consists of four integrated phases: (1) field data collection and model validation; (2) generation and simulation of urban canyon scenarios combining key geometric and shading variables; (3) evaluation of the modified Physiological Equivalent Temperature (mPET) index using a pre-trained machine learning model; and (4) comparative analysis to rank scenario performance. This combinatorial approach is used to provide design guidance based on descriptive analysis.

Study area

The study area is located in Nagpur City. It is the winter capital of Maharashtra state, situated in central India (21.1458° N, 79.0882° E). It is characterized by a tropical savannah (Aw) type of climate as per Koppen climate classification. Nagpur is known for extreme annual temperature variability, with recorded lows of 4°C in winter (December-February) and highs reaching 48°C during the summer (March-May). May is the hottest month with an average maximum air temperature of about 42°C. These hot summers frequently feature severe, city-wide heatwaves (ICLEI, 2021). The selection of New Shukrawari Street in Nagpur as a case study is based on the following criteria: Mixed land use on the street and in the neighbourhood, availability of a metro station for better connectivity, and availability of pedestrian sidewalks on both sides of the street. The street was 20 m wide and 1000 m in length, the average AR on the street was 0.8, and the SVF was 0.65.

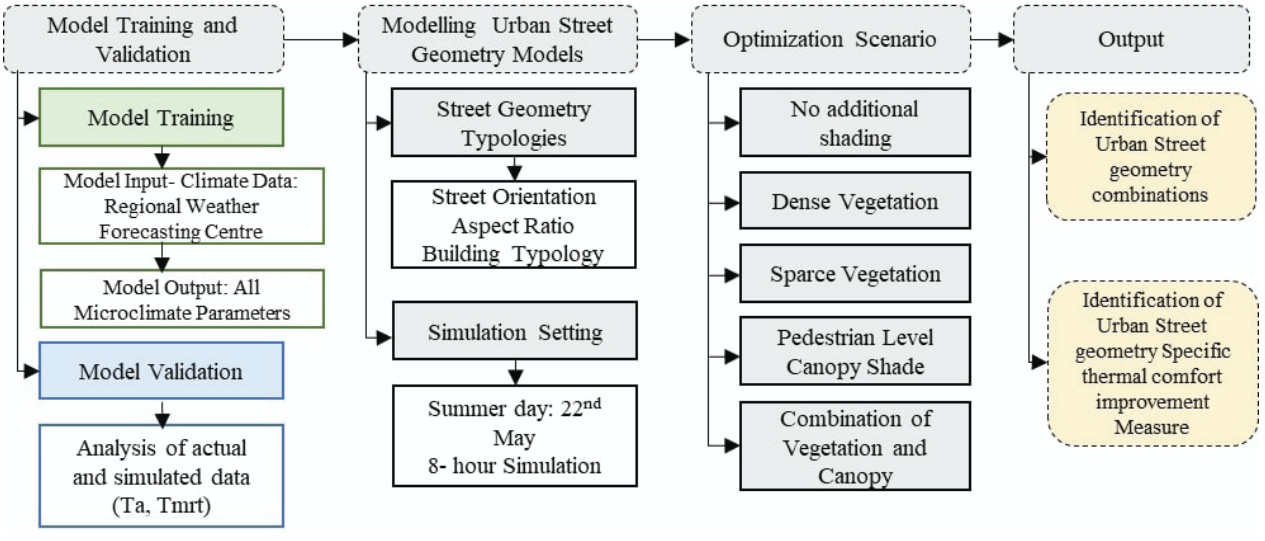

Figure 1. Proposed methodology for the study

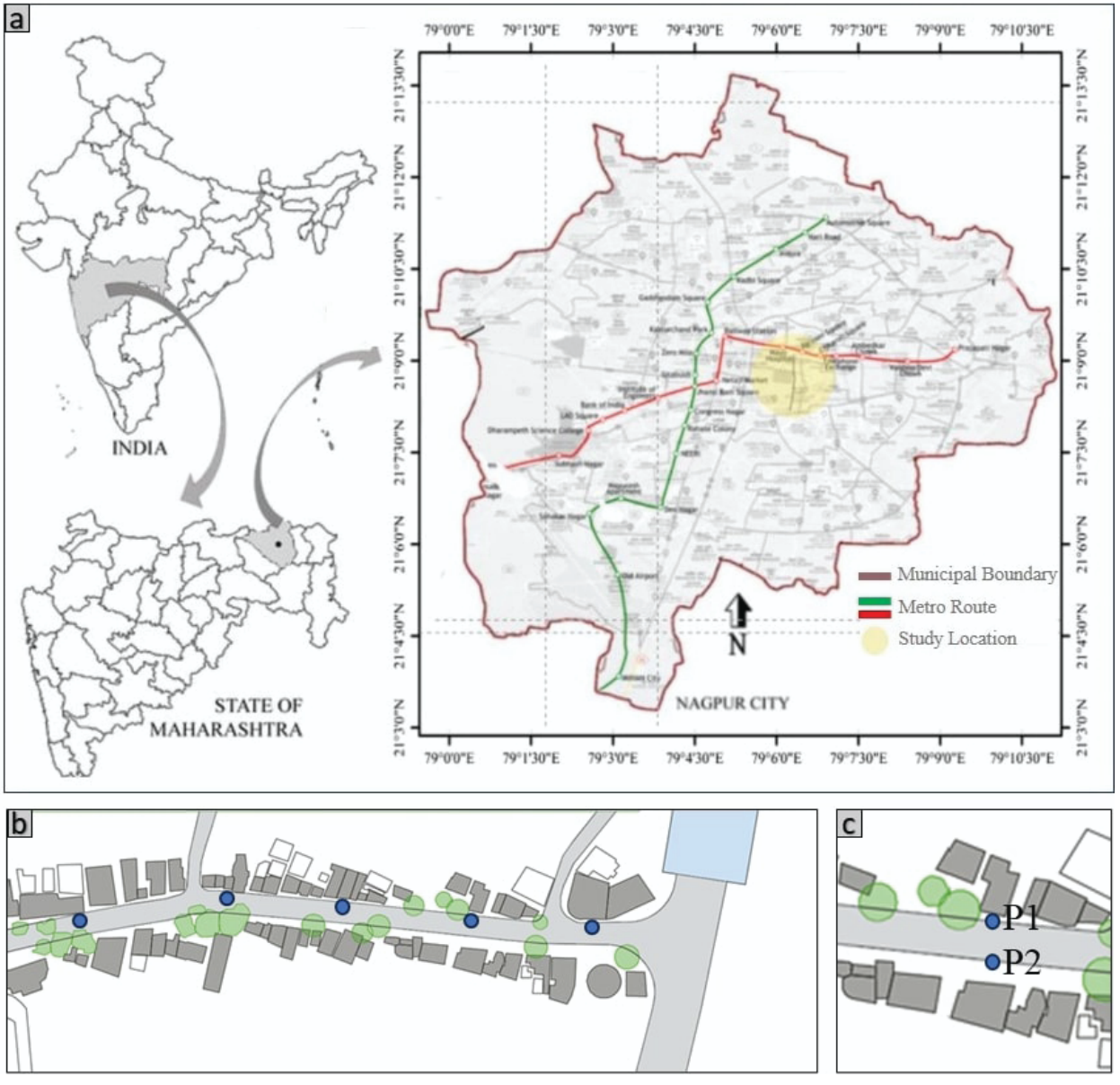

Figure 2. a. Location of Nagpur city with the studied location (Source: Meshram, 2011), b. Studied location: New Shukrawari Street, c. Points studied for validation.

Data collection and analysis

The field survey was conducted on May 22, 2022, under typical summer conditions, i.e., hot sunny days and cloudless. The data collection includes mapping of both street geometry and microclimate data. The microclimatic parameters (Ta, Rh, Ws) were measured at 1.2 m above the ground level, as it's the center of gravity of a standing human (ISO 1998). The data were collected at four different time slots between 09:00 and 18:00. To collect data, the street was divided into a grid of 100 m, and the data was collected on both sides of the street. The microclimate data was collected using MS6252B digital anemometer (Ta, Rh, Ws) and Lazer IR thermal gun (Ts). The street geometry data was collected using a Nikon DSLR with a fish-eye lens. The field data was then evaluated for Tmrt and mPET index using RayMan pro tool (Matzarakis, 2009). The mPET enhances accuracy of thermal comfort assessment by considering thermo-physiological parameters of the human body and climatic factors. Unlike other indices, mPET incorporates a multi-node heat transport model and a self-adapting multi-layer clothing model, providing a more realistic analysis of the impact of climate on humans (Pecelj et al., 2021). This particular index is used and validated in previous part of this study (Mohite & Surawar, 2024c). RayMan requires all microclimate parameters along with the fish eye lens image as input. The microclimate data and mPET values of the studied street are given in Table 1.

Table 1. Observed Values of Microclimate and thermal comfort index -mPET

Location	Time		Ta	Ts	RH	Ws	MRT	mPET
New Shukrawari Street	9 am-10 am	East	37.4°C	40.7°C	32.64%	0.91m/s	54.7°C	38.9
		West	38.1°C	45.8°C	32.07%	0.62m/s	58.9°C	40.6
	11.30 am -12.30 pm	East	42.9°C	57.3°C	24.68%	0.7m/s	57.5°C	42.3
		West	42.9°C	57.2°C	24.84%	0.67m/s	61.4°C	43.3
	2.30 pm -3.30 pm	East	41.7°C	56.4°C	25.7%	1.64m/s	64.5°C	44.1
		West	41.3°C	54.1°C	25.7%	1.04m/s	59.6°C	42.5
	5 pm-6 pm	East	38.9°C	52.5°C	24.6%	1.04m/s	53.0°C	41.2
		West	40.0°C	49.4°C	25.2%	1.19m/s	47.15°C	38.0

Simulation setting and model validation

ENVI-met 5.6.1 microclimate modeling software is used to simulate three-dimensional surface–air interaction representing the proposed scenarios in the study (Fig. 3a). This simulation method was previously used in various microclimate studies and has shown the credibility of the ENVI-met model. For instance, Ma et al. (2020) reported a slight variation between simulated and measured values of Ta, with R^2 values ranging from 0.76 to 0.98. Galal et al. (2020) found that the simulated Ta closely matched the measured diurnal temperature, achieving an index of agreement (IA) ranging from 0.96 to 0.98. Elnabawi et al. (2013) demonstrated a strong correlation for the anticipated mean radiant temperature (Tmrt) up to sunset (6:00 PM).

In this study, the model was validated by simulating the partial area of the surveyed street. Two measurement points were selected (P1 and P2) to simulate the model using local weather station data of May 2022 and record the model output for microclimatic (Ta, Ts, Tmrt) and urban geometry parameters (SVF) (Fig. 2). Ta and Tmrt play a major role in determining the performance of the accuracy analysis. The simulation process was run on May 22, 2022, on a typical hot day of the hottest summer month. May is the month with the most sunshine, with 11.8 hours of sunshine per day, and it has maximum Ta and Tmrt. During this month, Nagpur City has experienced heatwaves for the past 30 years, as per IMD data (Surawar et al., 2017). The simulation began at 10:00 a.m. since the morning hours of summer days stimulate a slight warm-to-

ENVI-met Model

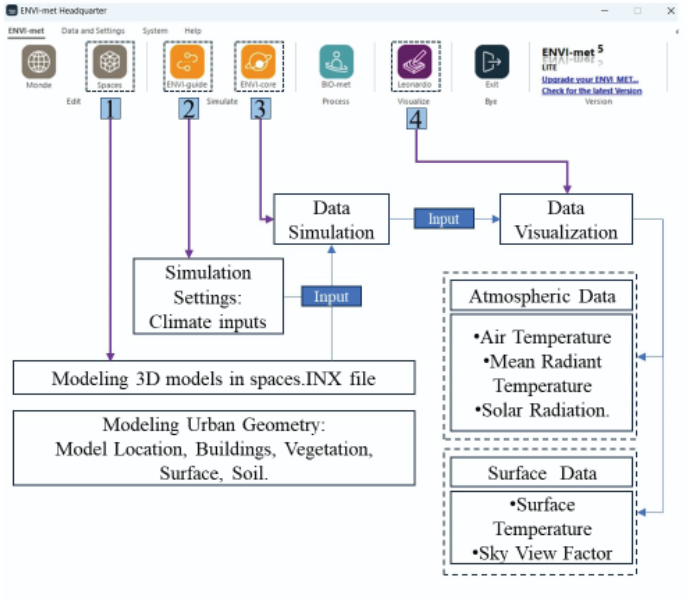

ENVI-met Model: Simulation Settings

Location	Nagpur, Maharashtra, India
Geographical Location	21.1458° N, 79.0882° E
Climate Type	Tropical savannah (AW)
Total Simulation Duration	8 hours
Spatial resolution	1m X 2m X 1m
Model Dimension (Number of grid cell)	X = 50, Y= 50, Z= 40
Date	22nd May, 2022
Building Material	Concrete Wall
Sidewalk Material	Concrete pavement Light
Vegetation Specification	
Type	Evergreen tree
Tree Height	6m
Crown Width	6m
Basic Meteorological Inputs	
Wind Speed	2.8 m/s
Wind Direction	295°C
Air temperature for 24h	Simple Forcing
Relative Humidity for 24h	Simple Forcing
Maximum air temperature	42°C
Minimum air temperature	30°C
Maximum relative humidity	48°C
Minimum relative humidity	22°C
Sky Condition	Clear Sky

Figure 3. ENVI-met model (a) and Simulation Setting (b)

warm thermal sensation (Mohite & Surawar, 2024a). The simulations were run for 8 hours until sunset to assess the data. The simulated weather data were obtained from the Regional Weather Forecasting Centre in Sonegaon, Nagpur. The mean values of Ta, RH and Va were utilized as input parameters for the ENVI-met simulation model. The models examined via ENVI-met had 50 × 50 × 40 grid units with a suitable resolution of 1 × 2 × 2 m grid. The input data for materials, vegetation, and microclimate is given in the table. Results are extracted for a height of 1.2 m (K=5) on the sidewalk, representing a standing person to evaluate the comfort degree for outdoor space users (Fig. 3b).

In order to evaluate the performance of the model, various statistical parameters were used in the calibration of the observed (O) and predicted (P) data. These statistical parameters include the agreement index (d), the coefficient of determination (R^2), mean bias error (MBE), and mean absolute error (MAE). This agreement index method, developed by Willmott in 1982, uses a specific formula for analysis (Willmott, 1982). The agreement index (d) is a descriptive measure indicating the extent to which the simulated values are free from error, ranging from 0 to 1. A value of 1 signifies perfect agreement, meaning the simulated values (s) are identical to the observed values (o). As the first indicator, the agreement index (d) ranges from 0 to 1, with values closer to 1 indicating higher accuracy. The higher coefficient of determination (R^2) value represents that the differences between the observed data (O) and the predicted data (P) are smaller and unbiased. The mean bias error (MBE) shows whether the values from the model are higher or lower than the observed data. The mean absolute error (MAE) is the same as the MBE indicator but takes into account the absolute difference between predicted and observed values (Battista et al., 2023). The MBE/MAE value must be between 0 and 1. If this value is 1 or close to 1, it shows the accuracy of the model.

These statistical parameters are calculated using the following equations:

$$d = 1 - \frac{(\sum_{i=1}^{n} (O_i - P_i)^2)}{(\sum_{i}^{=1n} (|P_i - \bar{O}| + |O_i - \bar{O}|)^2)} \quad , 0 \leq d \leq 1$$

(Equation 2)

$$MAE = (1/n) \times \sum_{i=1}^{n} |O_i - P_i|$$

(Equation 3)

$$MBE = (1/n) \times \sum_{i=1}^{n} (P_i - O_i)$$

(Equation 4)

Where,
d: Index of agreement
MAE: Mean absolute error
MBE: Mean bias error
ND: Number of analysed data
Ō: Mean of the observed variable
Oj: Observed variables for each instant j
Pj: Model-predicted variables for each instant j

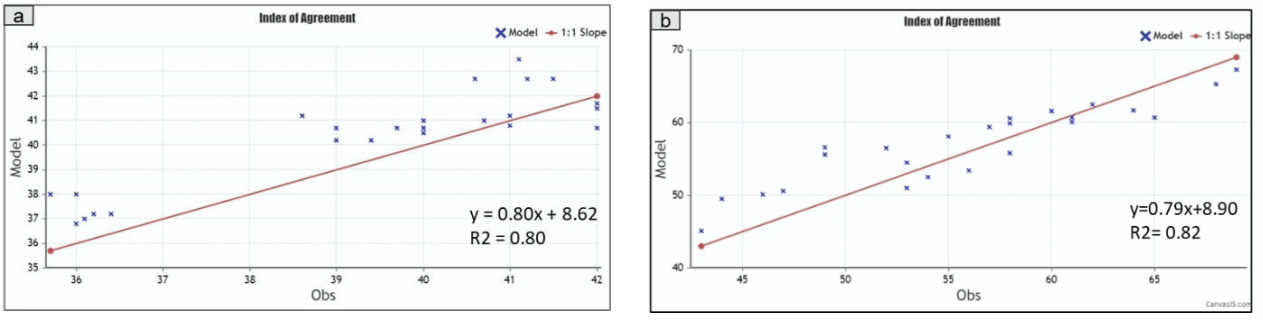

Figure 4. Results of model validation using the Index of Agreement (a) Air Temperature (b) Mean radiant temperature

The observed (O) and the predicted (P) values indicate the coefficient of determination (R^2) for Ta is 0.80, and R^2 for Tmrt is 0.82. In the analyses, the R^2 is very close to 1, which shows that they are statistically significant. In addition, the fit index (d) was determined as 0.85 for Ta and 0.89 for Tmrt (Fig. 4). The MBE and MAE for Ta are 0.92 and 1.44, respectively, whereas for Tmrt they are 0.73 and 1.02. These results show that the software has been well verified and the work can be run with these software outputs.

Modelling Street Geometry and Proposed Scenarios

The proposed scenarios are identified considering the primary factor affecting PTC: solar exposure. To reduce solar exposure on the pedestrian level, natural and artificial shading strategies are considered, which include shading through buildings, vegetation, pedestrian canopy, and a combination of vegetation and canopy. The study has considered two orientations (N-S and E-W), three ARs (shallow, uniform, and

deep), and three building typologies (singular, linear, and scattered) for simulation. The ARs considered in this research are consistent with the prior part of the research (Mohite & Surawar, 2024c), with the primary considerations such as: if AR of a street canyon is below 0.5, the canyon is considered shallow, if it is approximately equal to 1, the canyon is considered uniform; and if the AR is equal to or more than 2, the canyon is considered deep, being maintained. The considered setbacks between adjacent buildings vary with building typologies, ranging from no setback for linear buildings to 4M in singular buildings and 14M in scattered buildings. The building length is 20 m; these considerations are based on the studied streets in the prior part of the research. The scenarios were designed by permuting three geometric factors and five shading strategies, resulting in 90 combinations (2 Orientations × 3 Aspect Ratios × 3 Building Typologies × 5 Shading Strategies) that are considered for simulation in ENVI-met (Fig. 5 and 7).

a. Singular building typology with H/W of (shallow, uniform, and deep), two street orientations (N–S, E–W), and five mitigation scenarios (models 1 to 30);

b. Linear building typology with H/W of (shallow, uniform, and deep), and two street orientations (N–S), and five mitigation scenarios (models 31 to 60);

c. Scattered building typology with H/W of (shallow, uniform, and deep) and two street orientations (N–S), and five mitigation scenarios (models 61 to 90).

The building material was specified as concrete, reflecting common construction in Nagpur, with an albedo of 0.3. Vegetation was modeled using the evergreen tree profile within ENVI-met, with a height and crown width of 6m. Canopies were modeled as horizontal planes at 3m height.

For all scenario simulations, a consistent protocol was followed to ensure comparability. Each of the 90 scenarios was simulated for 8 hours, considering climate of May 22, 2022 (10:00 a.m.–6:00 p.m.). Microclimate data for PTC analysis was extracted for every hour and the average for entire period was considered for comparison. To ensure data representativeness, output parameters (microclimate data) were extracted at 1.2 m height for ten receptor points per sidewalk (points were positioned at 10m intervals on either side), and then average was considered (Fig. 6).

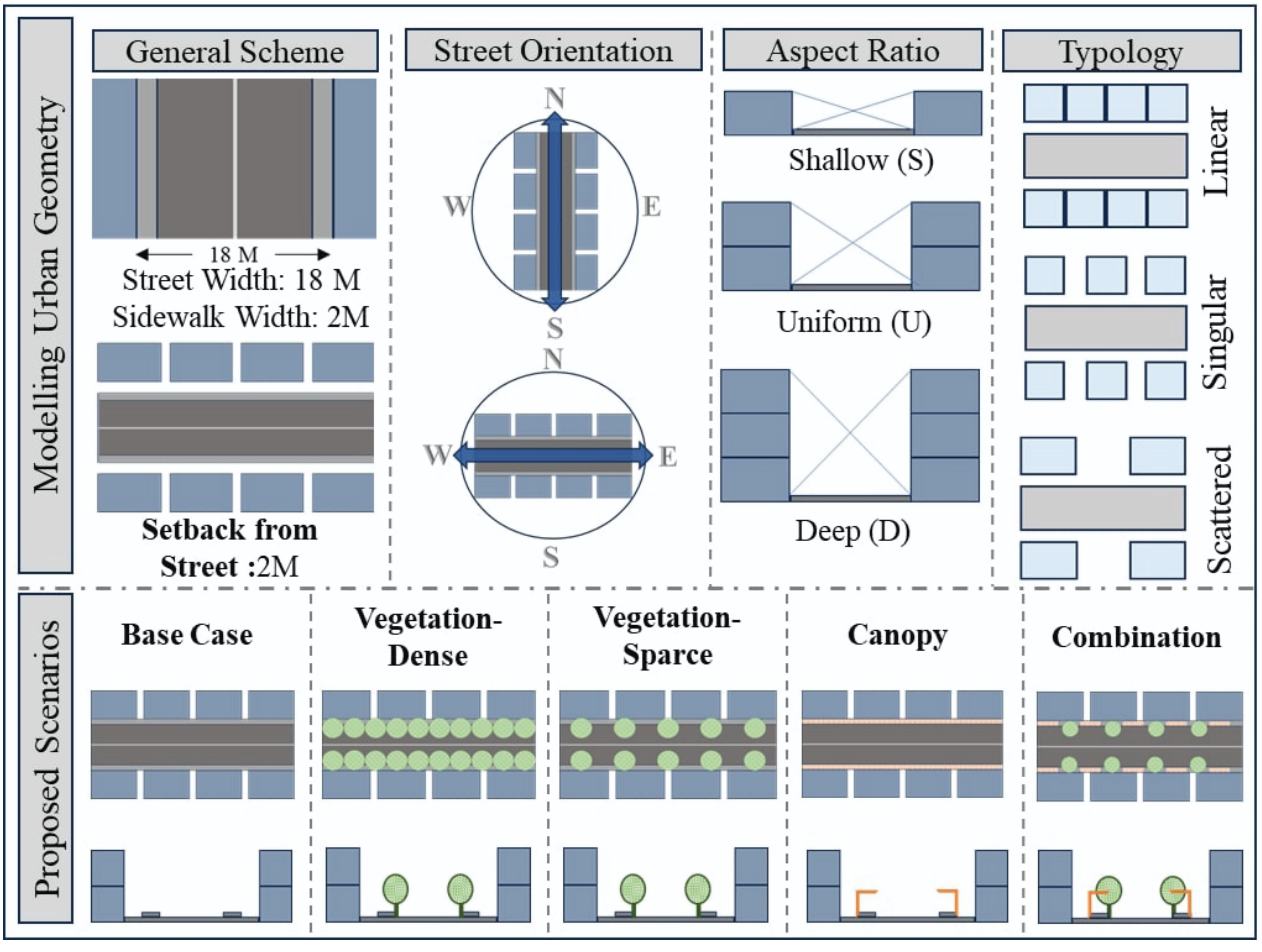

Figure 5. Proposed urban street geometry and shading strategies for the study

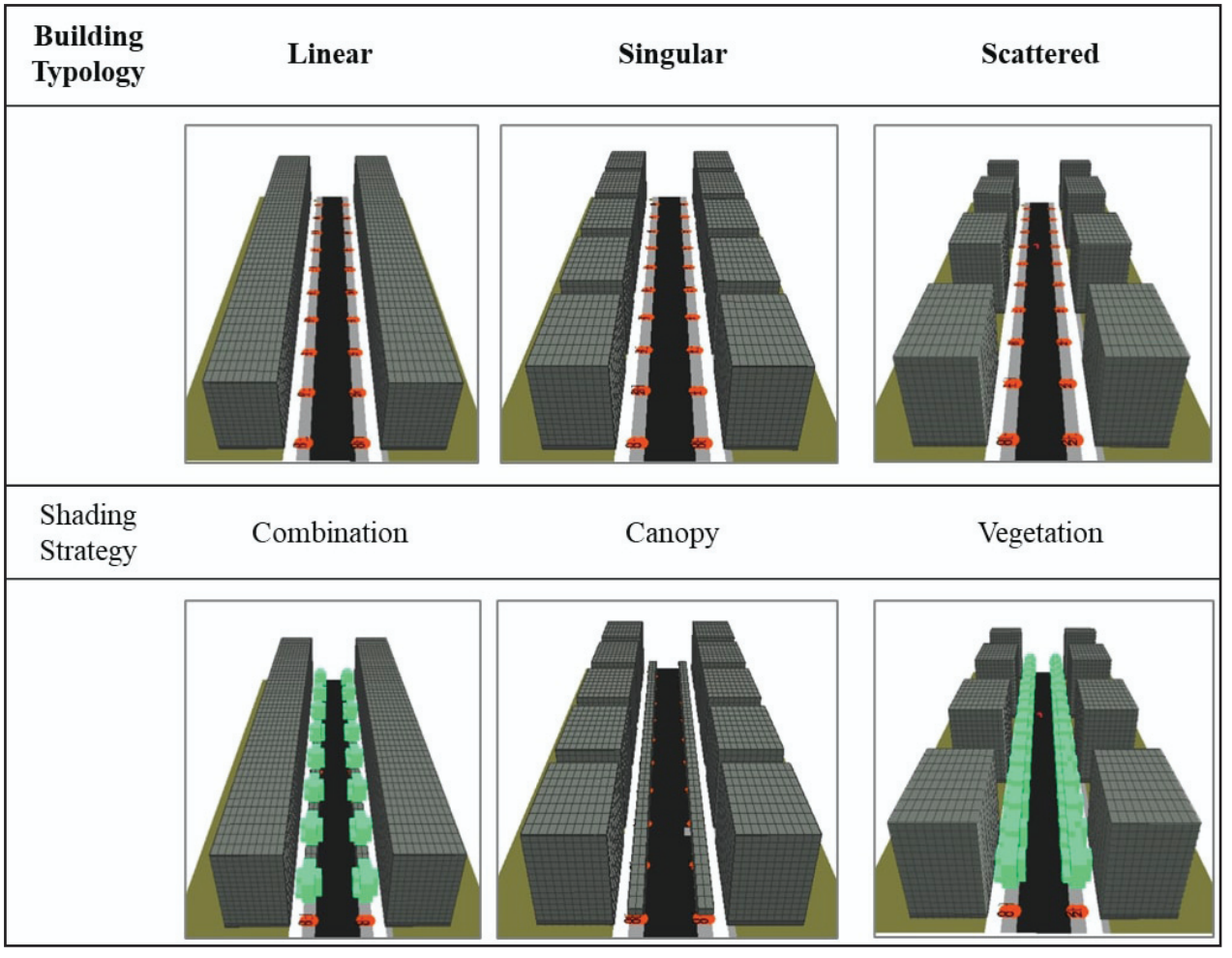

Figure 6. The Representative space setting input files of the ENVI-met 3D model: a) Base case with three building typologies; b) three representative shading strategies- vegetation, canopy and combination

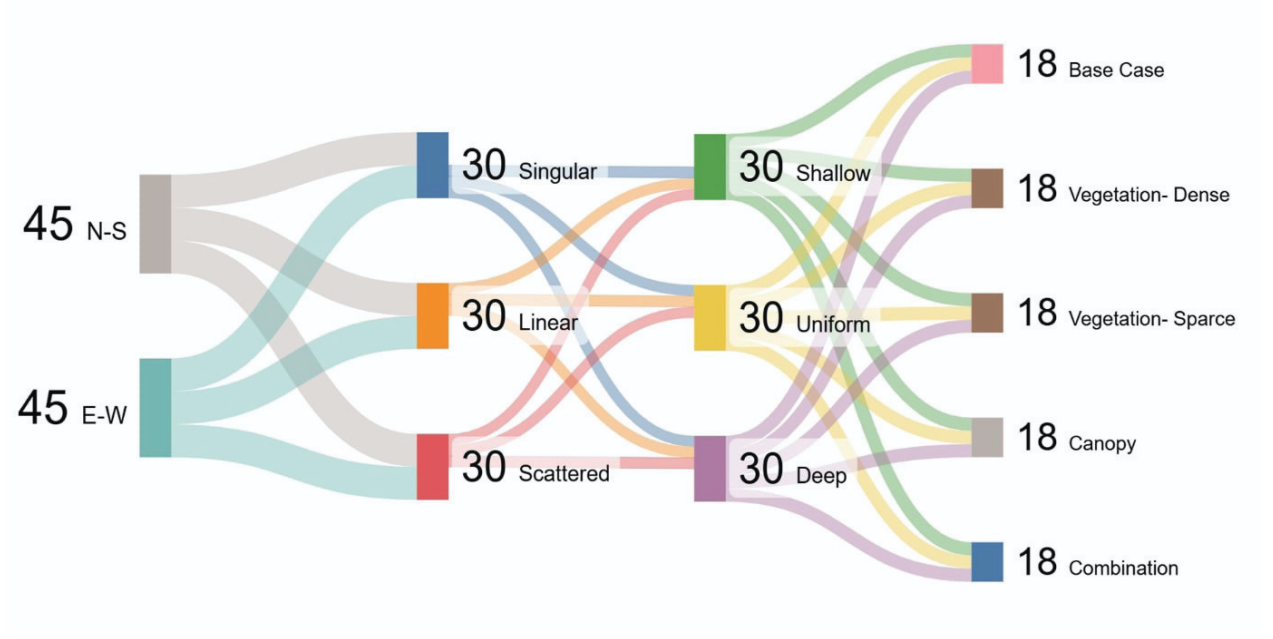

Figure 7. Designed combinations of urban street geometry and shading strategies

Evaluation of mPET values

In the previous part of this study, a machine learning model was developed using Random Forest (RF) algorithm for assessing and predicting PTC. The model was trained using urban geometry and microclimate data (Mohite & Surawar, 2024b). The model was validated for unseen data and showed a high level of accuracy ($R^2 > 0.90$ at training phase and $R^2 > 0.80$ at prediction phase, low mean squared error values - overall MSE < 1.4). Thus, in this study, the pre-trained RF model was used to evaluate mPET alongside of the street, using the microclimate parameters from the simulated model. The model utilizes simulated hourly values of Ta and solar radiation from ENVI-met outputs, along with the predefined SVF and AR for each scenario, were given as input into this model to generate corresponding mPET values at the receptor points (Fig. 1). These mPET values are then used for analyzing the influence of urban geometry and shading strategies.

Results

Influence of Aspect Ratio and Street Orientation

The AR is essential in shaping PTC by influencing solar exposure, shading, and wind movement within urban streets. The effects vary significantly depending on the street orientation. Shallow street canyons, characterized by an AR of 0.5 or lower, exhibit poor shading due to their low building heights relative to street width. In N-S-oriented shallow streets, maximum exposure to solar radiation leads to mPET values ranging between 36.9°C and 42.9°C. Similarly, Shallow E-W streets experienced the highest mPET values, ranging from 37.9°C to 43.9°C.

Uniform street canyons, with an AR close to 1.0, offered better thermal comfort than shallow canyons. In N-S oriented uniform streets, mPET values ranged from 34.1°C to 41.4°C, representing a reduction of 2–3°C compared to shallow N-S streets. In E-W uniform streets, mPET values drop by 1-2°C compared to their shallow counterparts, ranging from 35.1°C to 43.3°C. However, persistent solar exposure in E-W orientations keeps thermal conditions in the "hot" to "very hot" range on the mPET index, highlighting the limitations of this orientation despite improved AR.

Deep street canyons, with an AR of 1.2 or higher, offer the most significant improvements in thermal comfort by maximizing shading. N-S-oriented deep AR streets achieve the lowest mPET values, ranging from 33.1°C to 40.1°C. On-E-W-oriented street as increased building heights provided marginal improvements, with mPET values ranging from 35.8°C to 43.2°C.

The interaction between AR and street orientation is essential in determining thermal comfort. Shallow canyons, particularly in E-W orientations, perform poorly, leading to mPET increases of up to 3-4°C compared to deep canyons. Uniform canyons provide moderate improvement, especially in N-S orientations, though E-W orientations still experience thermal stress. Deep canyons offer the best thermal performance, particularly in N-S orientations, where mPET values are significantly lower. However, E-W deep canyons remain thermally challenging due to persistent solar exposure (Fig. 7).-

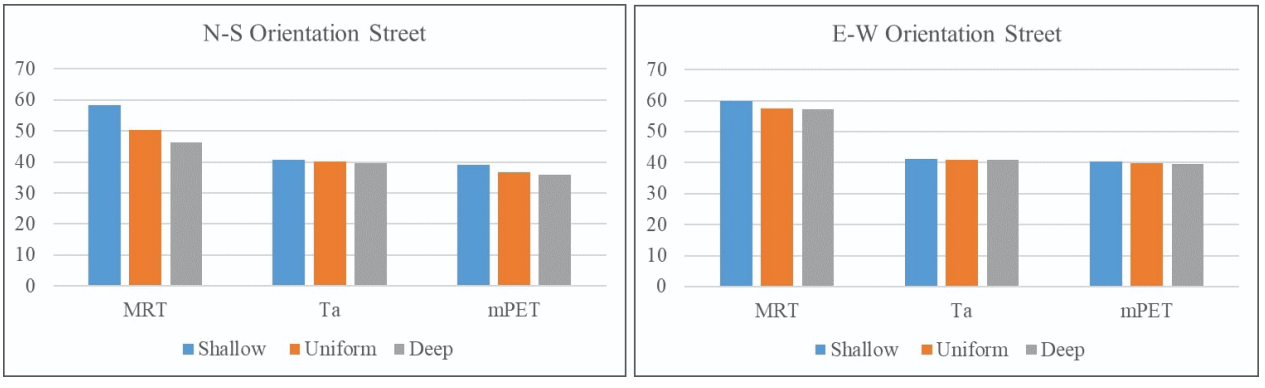

Figure 8. Influence of Aspect Ratio and Street Orientation on Microclimate and mPET Index

Influence of Building Typology on Thermal Comfort

The BSF for each building typology was evaluated using Equation 1. The linear typology depicts dense building typology having no gaps in buildings; these typologies have a BSF value of 1; the singular typology has minimum setbacks between buildings and has a BSF value of 0.84. The scattered typology has high gaps between buildings, leading to a BSF value of 0.57.

N-S Orientation

For N-S-oriented streets, the linear typology (BT2) remains the best performer across all scenarios, as minimum Ta (39.7°C) and Tmrt (48.5°C) were observed. This typology has the highest BSF values, creating continuous street canyons that limit solar penetration and maintain consistent shading on the southern side of the street throughout the day. The singular typology (BT1) shows higher Tmrt (50.8°C) and Ta (40.15°C) values than linear typologies. The scattered typology (BT3) performs worst for N-S streets, primarily due to the large setbacks between buildings, leading to low BSF values. These open spaces allow for continued solar exposure, leading to increased Tmrt values (56.2°C) and increased Ta (41.8°C) (Fig. 8a).

E-W Orientation

For E-W-oriented streets, solar exposure and its impact on Tmrt are more pronounced due to their alignment with the sun's path. The singular typology (BT1) is the most thermally favorable option, with reduced Tmrt (56.2°C) and Ta (40.8°C) values compared to other typologies. The linear typology (BT2) also performs better, with slightly higher Tmrt (57°C) and Ta values (40°C) compared to singular typologies. The scattered typology (BT3) exhibits maximum mPET values in E-W streets. The large setbacks exacerbate solar exposure, leading to the highest Tmrt (58.5°C) and Ta (58.5°C) values across all typologies (Fig. 8b).

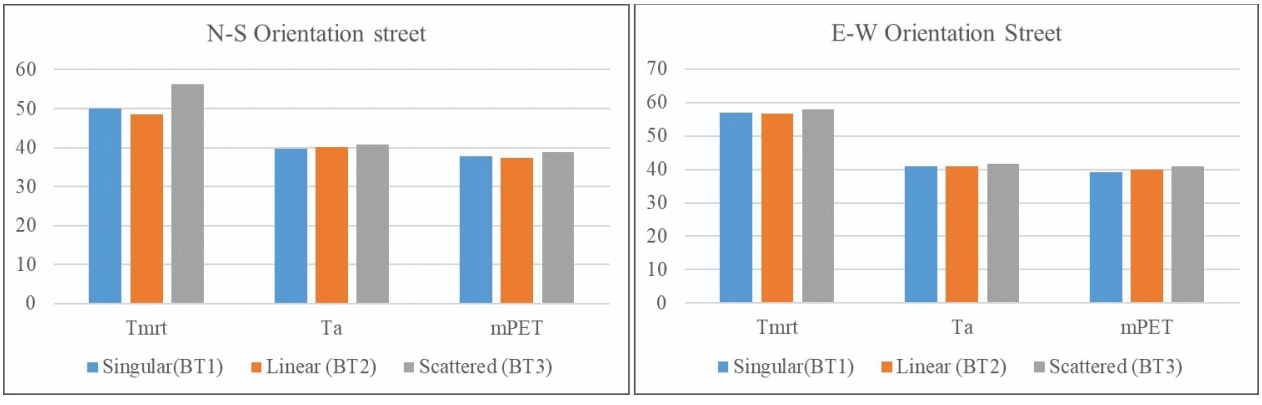

Figure 9. Influence of Building Typology on Microclimate Parameters and mPET index- (a: N-S-Orientation Street, b: E-W-Orientation Street)

Proposed Shading Scenario

The thermal performance analysis on two different street orientations reveals distinct variations in outdoor thermal comfort due to differences in solar exposure and urban configurations.

N-S oriented streets

In the base case scenario, where there was no vegetation or canopy, street geometry heavily influenced the thermal environment. For singular building typologies, mPET values ranged from 38.28°C on the west-facing sidewalk in deep AR to 41.5°C on the east-facing sidewalk in shallow AR. For Linear typologies, on the other hand, displayed mPET values ranging between 37.8°C (west-facing sidewalk) and 42.2°C (east-facing sidewalk). Scattered typologies recorded the highest mPET values, with all AR configurations reaching up to 42.9°C.

The sparse vegetation (4m apart) provides minor cooling benefits. For singular building typologies, the mPET was reduced to 37.28°C on the west-facing sidewalk in deep AR and 41.3°C on the east-facing sidewalk in shallow and deep AR. Linear typologies experienced slightly better thermal performance, with mPET ranging from 36.7°C to 41.0°C. Scattered typologies showed a slight reduction in mPET, ranging from 37.9°C to 41.5°C.

Dense vegetation shows significant improvement in thermal comfort across all typologies, particularly in deep AR. In singular building typologies, the mPET reduced further to 34.2°C on the west-facing sidewalk of deep AR and 39.9°C on the east-facing sidewalk of shallow AR. Similarly, in linear typologies, mPET values ranged from 34.9°C to 40.3°C, with deep AR benefiting the most from dense vegetation's shading and cooling-enhancing effects. For scattered typologies, while dense vegetation led to mPET reductions ranging from 36.9°C to 40.6°C, the irregular shading distribution limited its potential to create uniform cooling.

The canopy shading shows improved values of mPET in all AR's. For singular building typologies, mPET decreased to 34.2°C on the west-facing side-

walks of deep ARs and 38.4°C on the east side of shallow layouts. Canopies provided consistent shading and effectively blocks direct sunlight. Linear typologies benefited the most, with mPET values ranging from 33.1°C to 38.2°C. Scattered typologies, while benefiting from canopies, recorded slightly higher mPET values ranging between 35.5°C and 38.6°C due to the irregular shading distribution.

The combination of vegetation and canopies proved to be an effective strategy for improving thermal comfort in N-S-oriented streets. For singular building typologies, the mPET decreased to 34.28°C in deep layouts and 39.94°C in shallow ARs. Linear typologies exhibited consistent cooling benefits, with mPET values ranging from 33.8°C to 39.3°C, as the combination of vegetation and canopies ensured even shading and reduced heat accumulation. Scattered typologies displayed improvements with mPET ranging from 36.3°C to 40.1°C, but they still lagged slightly behind singular and linear typologies (Fig. 9).

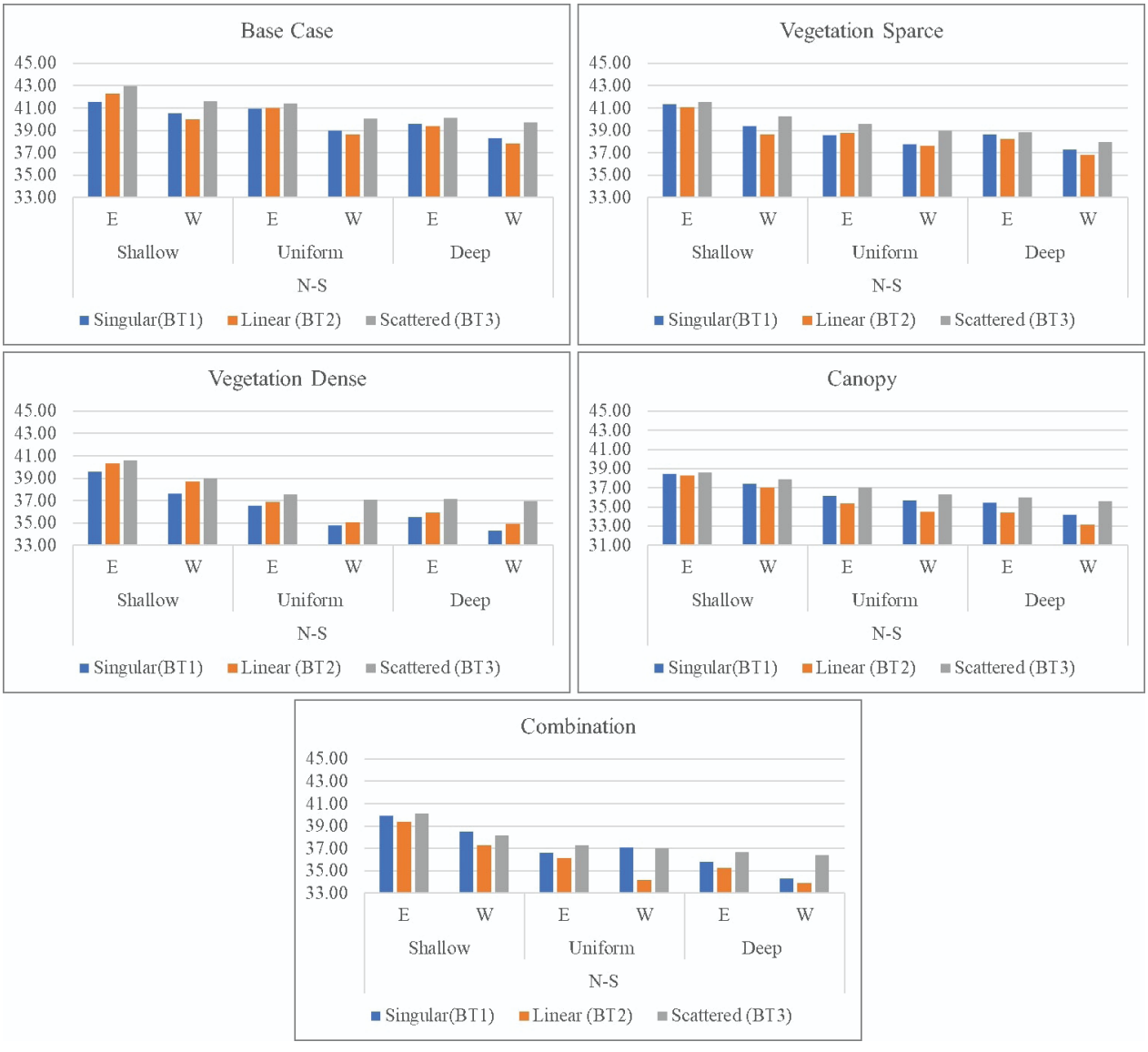

Figure 10. Comparison of Effect of no-shade and shading strategies on mPET on N-S-Orientation Street

E-W streets

For E-W-oriented streets, mPET was significantly influenced by building typology and shading interventions, and side of the street. In the base case scenario, the mPET values reflected the direct impact of the sun's trajectory. For singular building typologies, mPET values ranged from 43.40°C on the shallow north-facing sidewalk to 41.9°C on the deep south-facing sidewalk. The north-facing sidewalk consistently exhibited higher mPET values (43.2°C), while the south-facing

sidewalk had relatively lower values (42.5°C). The linear typology (BT2) demonstrates mPET values varying between 43.9°C on the north-facing sidewalk and 42.5°C on the south-facing sidewalk. Scattered typologies recorded the highest mPET values, ranging from 43.2°C south-facing sidewalk to 44°C on a north-facing sidewalk, especially in shallow and uniform configurations.

With sparse vegetation, the result shows a slight reduction in mPET values. For the singular typology (BT1), mPET decreases by approximately 2.5°C to 3°C, ranging between 40.8°C on the south- facing sidewalk of deep AR and 40.12°C on the north-facing sidewalk of shallow AR. The linear typology (BT2) achieves a reduction of around 2°C to 3°C, ranging from 42.2°C to 40.3°C. The scattered typology (BT3) exhibits similar reduction, ranging between 42.7°C and 40.7°C.

Dense vegetation considerably improves thermal comfort in E-W streets. In singular building typologies, mPET values further decreased to 38.97°C on the south side of deep AR and 38°C on the north side of shallow AR. Similarly, the linear typology (BT2) records temperatures between 40.4°C and 38.4°C, while the scattered typology (BT3) registers values ranging from 40.9°C to 38.7°C. The overall reduction is approximately 4°C to 5°C compared to the base case scenario.

With the canopy shading scenario, the singular typology (BT1) records the lowest mPET values, ranging from 37.6°C to 35.04°C, achieving a reduction of approximately 6°C to 7°C compared to the base case. The linear typology (BT2) ranged from 38.6°C to 36.3°C, while the scattered typology (BT3) records values between 38.3°C and 37.2°C.

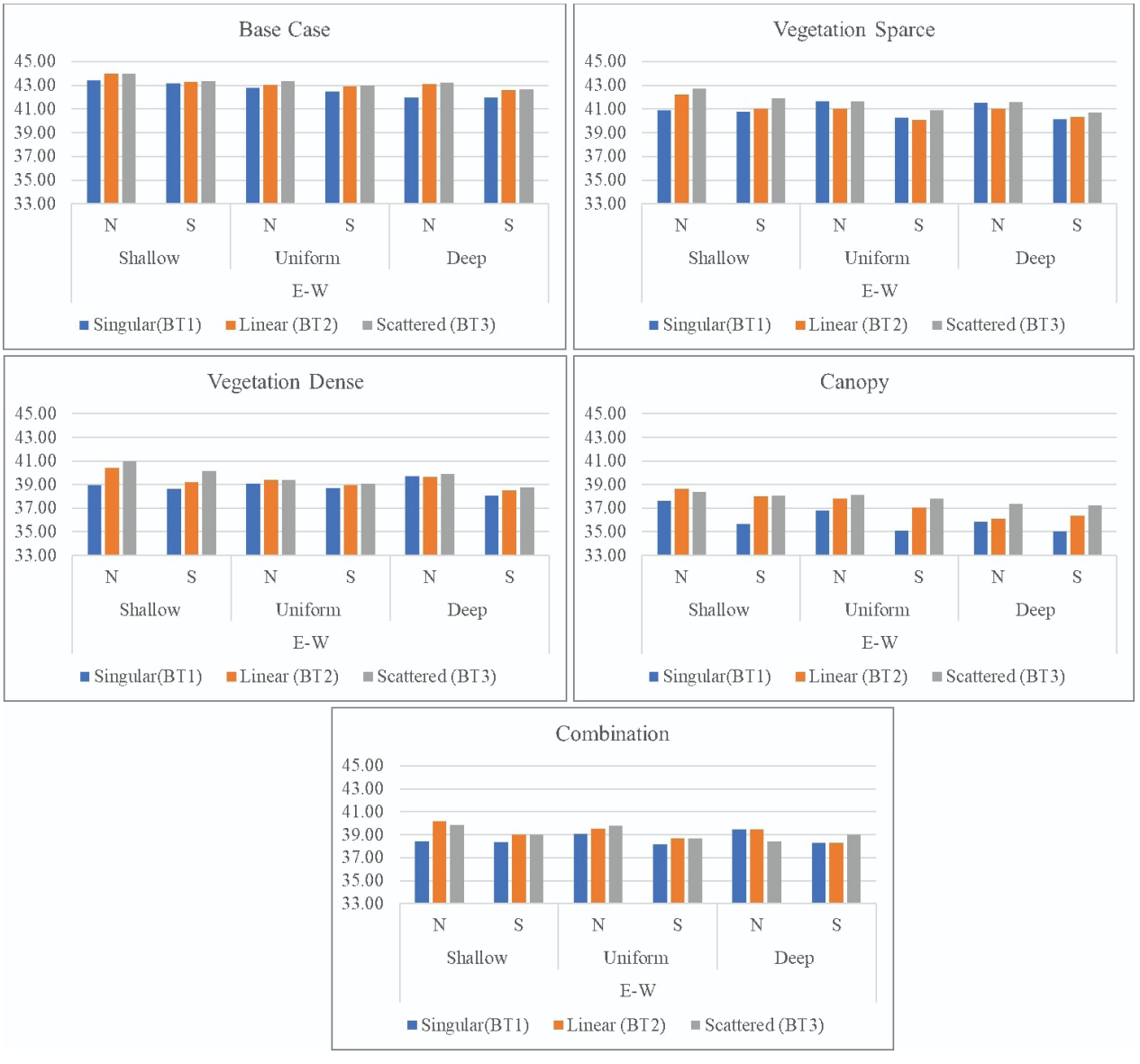

Figure 11. Comparison of the Effect of No-Shade (base case) and Shading Strategies on mPET on E-W-Orientation Street

The combination of vegetation and canopies emerged as an effective strategy for mitigating heat stress in E-W streets. It significantly reduces mPET values across both south- and north-facing sidewalks. The singular typology (BT1) records mPET values ranging from 38.4°C to 38.1°C, indicating reductions of over 5°C to 7°C compared to the base case. Similarly, the linear typology (BT2) ranged between 40.1°C and 38.3°C, while the scattered typology (BT3) records values ranging from 39.8°C to 38.9°C (Fig. 10).

Identification of Street-Specific Shading Strategies

The comprehensive analysis of ENVI-met results for all 90 scenarios provided critical insights into the effectiveness of various shading strategies in enhancing thermal comfort on urban streets. Each strategy provided a different level of thermal comfort improvement; thus, each strategy was evaluated using a detailed rating system. The mPET values are categorized into ratings based on the accepted thermal comfort range for summer, identified earlier in the study as 24.1°C–36.8°C (Mohite & Surawar, 2024a). The observed thermal comfort ranges from this study were then divided into 5 equal categories. Ratings 4 and 5 fall within this thermal comfort range, while ratings 1, 2, and 3 represent increasingly warmer conditions beyond the comfort zone. The rating categories are as follows:

Table 2. Categorization of mPET Values into Thermal Comfort Ratings

Rating	mPET Range (°C)	Range of Thermal perception as per mPET
5	33.8–35.82	Slightly warm - warm
4	35.82–37.84	Warm
3	37.84–39.86	Hot
2	39.86–41.88	Hot
1	41.88–43.9	Very Hot

Source: Matzarakis & Mayer, 1996; Lin & Matzarakis, 2008; Mohite & Surawar, 2024a

The evaluation accounted for variations in street orientation, AR, and BT, providing an understanding of the performance of shading strategies under diverse urban conditions, as illustrated in Table 3.

In N-S-oriented streets, vegetation and canopy shading consistently performed better. In contrast, on E-W-oriented streets, canopy shading was more effective due to its ability to block direct solar radiation as the sun travels along its path. The effectiveness of dense vegetation in N-S streets varied, with ratings typically between 2 and 5 and often achieving ratings of 4 and 5. This higher efficiency was particularly noted in streets with higher AR values and compact building typologies, where the interaction between urban geometry and greenery maximized shade coverage. For E-W streets, dense vegetation is effective, with scores ranging from 2 to 3. This reduced efficiency compared to N-S-oriented streets can be attributed to the sun's east-west movement, which limits the shading benefits during the early morning and late afternoon hours.

Canopy shading demonstrated similar orientation-based differences. N-S streets consistently received ratings of 4 or 5, as canopies provided continuous shading throughout the day by aligning with the solar path. In E-W streets, the effectiveness of canopies was slightly improved, with ratings ranging from 3 to 4, as shading coverage was uniform during certain times of the day, highlighting the orientation-specific interaction between canopy placement and sun angles.

In N-S-oriented streets, the Combination Strategy demonstrates performance levels similar to Dense Vegetation, achieving ratings between 3 and 5 across most configurations. This similarity can be attributed to the substantial shading provided by the interplay of tree and pedestrian-level canopies, which creates a stable microclimate, effectively reducing heat stress. However, canopy shading consistently outperforms both dense vegetation and the combination Strategy, receiving higher ratings. In E-W streets, the combination strategy performed high, with ratings of 3.

Sparse vegetation is moderately effective, scoring between 2 and 3 on N-S, whereas it scores 1 and 2 on E-W orientation. The sparse tree cover could partially mitigate heat during peak afternoon hours. However, sparse vegetation remained insufficient to meet the accepted thermal comfort range, demonstrating limited applicability for high-density urban areas or streets with higher AR values.

The analysis highlights that the highest-rated strategies (5) align with the accepted thermal comfort range but are fewer in number due to the inherent complexity of achieving thermal comfort solely through shading. This shows the need to consider other environmental factors, such as wind patterns, reflective materials, and the cooling effects of water bodies, to enhance the overall microclimate. While shading remains a critical component of thermal comfort, it must be integrated into a holistic urban design approach to achieve maximum efficiency.

The findings highlight the importance of horizontal shading solutions like canopies, particularly in E-W streets, where they provide the most effective mitigation against solar exposure. This analysis emphasizes the importance of modifying shading strategies to specific street characteristics and integrating them with complementary environmental interventions to create resilient and thermally comfortable urban environments.

Table 3. Thermal Comfort Evaluation Matrix Based on mPET Ratings Across Building Typologies and Vegetation Scenarios

Street Orientation	Aspect Ratio (AR)	Building Typology (BT)	Side of the Street	Base Case	Vegetation (Sparse)	Vegetation (Dense)	Canopy	Combination
N-S	Shallow	BT1 (Singular)	E	1	1	2	3	2
			W	2	3	3	3	3
		BT2 (Linear)	E	1	2	2	3	3
			W	2	3	3	4	3
		BT3 (Scattered)	E	1	1	2	3	2
			W	1	2	3	3	3
	Uniform	BT1 (Singular)	E	2	3	4	4	4
			W	3	3	5	5	5
		BT2 (Linear)	E	2	3	4	4	4
			W	3	3	4	5	5
		BT3 (Scattered)	E	1	2	3	4	3
			W	2	3	4	4	4
	Deep	BT1 (Singular)	E	2	3	4	5	4
			W	3	3	5	5	5
		BT2 (Linear)	E	3	3	4	5	4
			W	3	4	5	5	5
		BT3 (Scattered)	E	2	3	4	4	4
			W	2	3	4	4	4
E-W	Shallow	BT1 (Singular)	N	1	2	2	3	3
			S	1	2	3	4	3
		BT2 (Linear)	N	1	1	2	3	2
			S	1	2	3	4	3
		BT3 (Scattered)	N	1	1	2	3	2
			S	1	1	2	3	3
	Uniform	BT1 (Singular)	N	1	1	3	4	3
			S	1	2	3	4	3
		BT2 (Linear)	N	1	2	3	4	2
			S	1	2	3	4	3
		BT3 (Scattered)	N	1	1	2	3	2
			S	1	2	3	3	3
	Deep	BT1 (Singular)	N	1	1	3	4	3
			S	1	2	3	4	4
		BT2 (Linear)	N	1	2	3	4	3
			S	1	2	3	4	4
		BT3 (Scattered)	N	1	1	2	3	3
			S	1	2	3	3	3

Rating with respective mPET Ranges: **5**- 33.8–35.82; **4**- 35.82–37.84; **3**- 37.84–39.86; **2**- 39.86–41.88; **1**- 41.88–43.9

Discussion and Conclusion

This paper investigated the influence of urban street geometry and shading strategies on pedestrian thermal comfort through microclimate simulations using ENVI-met 5.6.1 and the mPET index evaluation using trained machine learning model. The study analyzed 90 urban scenarios, varying building typologies (singular, linear, scattered), aspect ratios (shallow, uniform, deep), street orientations (N–S, E–W), and shading interventions (vegetation, canopies, or combined). The simulation of 90 urban scenarios revealed that pedestrian thermal comfort (mPET) is most effectively improved through the synergistic integration of street geometry and targeted shading strategies, rather than either approach in isolation. The results support the critical role of street orientation in influencing outdoor thermal comfort, especially in hot climates. The N–S orientation consistently exhibited better thermal performance, as indicated by lower mPET values (Minimum up to 33.1°C) and reduced exposure to direct solar radiation during a significant duration of the day. These orientations benefit from prevailing wind direction, leading to increased wind velocity (Va), which plays a significant role in convective cooling. Whereas, E–W-oriented streets presented the most thermally stressful conditions, with mPET values peaking at 43.9°C, primarily due to elevated mean radiant temperatures (Tmrt) and significantly reduced wind flow. This is consistent with previous studies, (Elnabawi & Hamza, 2020; Elraouf et al., 2022; Mahmoud & Ghanem, 2019; Sharmin & Steemers, 2013), confirming the negative effect of E–W orientation on thermal comfort environment. The higher aspect ratio shows improved thermal comfort due to increased self-shading of the canyon walls, reducing Tmrt. This aligns with findings from other climatic contexts, (Achour-Younsi & Kharrat, 2016b; De & Mukherjee, 2018a, 2018b; Galal et al., 2020b; Lobaccaro et al., 2019; Qaid & Ossen, 2015c) supporting the use of shaded street profiles to mitigate solar radiation exposure. However, additional shading measures such as tree planting or overhead canopies are necessary, especially in E–W-oriented streets, where solar exposure remains high during afternoon hours regardless of aspect ratio(Mohite & Surawar, 2024c). The results also showed that the benefit of a deep aspect ratio is strongly moderated by orientation. While deep canyons provided the greatest improvement in N-S streets, their efficacy in E-W streets was limited, demonstrating that geometry alone cannot overcome the solar exposure inherent to east-west orientation.

The role of building typology further complements the findings on street geometry. The results align with (Abd Elraouf et al., 2022b; Abdollahzadeh & Biloria, 2021) indicated that the linear typology of buildings provides the highest level of comfort among the other alternatives. Meanwhile, the singular typology is the best option for E–W-oriented streets, as it generates the least Tmrt value and the highest Va value in these orientations.

Among shading strategies, canopy shading was most impactful, reducing mPET by up to 7°C, particularly in E–W streets where horizontal shading proved most useful. Dense vegetation also improved comfort but was less effective than canopies in E–W orientations due to solar path alignment.

This performance difference can be attributed to the distinct cooling mechanisms. Canopies provide continuous, horizontal obstruction of the sun's path, directly and consistently reducing Tmrt. Vegetation, while offering shading and evaporative cooling, casts dynamic, vertical shadows that provide less complete coverage against the low-angle morning and afternoon sun prevalent in E–W streets, explaining its relative lower efficacy in these orientations. The findings emphasize that optimal thermal comfort requires context-specific solutions. The thermal comfort rating matrix (Table 3) operationalizes this principle, providing a decision-support tool. It translates complex interactions into actionable guidance, showing, for example, that for an existing E–W street with a shallow aspect ratio, canopy shading (Rating 3-4) is a more reliable intervention than sparse vegetation (Rating 1-2).

While this study demonstrated the effectiveness of shading strategies in general, it was assumed that shading is either uniform or sparse considering fixed distance between two trees, along the entire street length. However, in reality, length, type of shading, placement, and frequency significantly influence localized thermal discomfort. This study focused on continuous shading elements and used wind data as a model input rather than analyzing ventilation interplay in detail. Future research should investigate the microclimate effects of various shade patterns, such as varying tree types, spacing or canopy gaps, on transient thermal perception.

Therefore, future studies may investigate the role of shading length and frequency by assessing localized skin temperature variations and transient thermal discomfort. This analysis may provide practical guidelines for optimizing shading distribution by ensuring consistent thermal comfort rather than relying solely on full-length shading solutions.

In conclusion, for the tropical savanna climate, development of thermally comfortable streets shall prioritize important actions such as actions favoring N–S orientations with deep canyons where possible,

and deploying extensive horizontal shading like canopies as the primary mitigation for unavoidable E–W streets. The findings and the rating matrix shows that effective design requires moving beyond generic solutions to strategically align geometric form with specific, climate-responsive shading interventions. Street designs that will enable pedestrians to walk around comfortably in terms of thermal comfort are important. People working in the planning and design discipline should conduct even more research on this subject. Especially in urban renewal and transformation areas, better space designs should be made for people by increasing their thermal comfort.

References

Abdelhafez, M. H. H., Altaf, F., Alshenaifi, M., Hamdy, O., & Ragab, A. (2022). Achieving Effective Thermal Performance of Street Canyons in Various Climatic Zones. *Sustainability*, *14*(17), 10780–10780. https://doi.org/10.3390/SU141710780

Abdollahzadeh, N., & Biloria, N. (2021). Outdoor thermal comfort: Analyzing the impact of urban configurations on the thermal performance of street canyons in the humid subtropical climate of Sydney. *Frontiers of Architectural Research*, *10*(2), 394–409. https://doi.org/10.1016/J.FOAR.2020.11.006

Achour-Younsi, S., & Kharrat, F. (2016a). Outdoor Thermal Comfort: Impact of the Geometry of an Urban Street Canyon in a Mediterranean Subtropical Climate – Case Study Tunis, Tunisia. *Procedia - Social and Behavioral Sciences*, *216*(October 2015), 689–700. https://doi.org/10.1016/j.sbspro.2015.12.062

Achour-Younsi, S., & Kharrat, F. (2016b). Outdoor Thermal Comfort: Impact of the Geometry of an Urban Street Canyon in a Mediterranean Subtropical Climate – Case Study Tunis, Tunisia. *Procedia - Social and Behavioral Sciences*, *216*, 689–700. https://doi.org/10.1016/J.SBSPRO.2015.12.062

Aghamolaei, R., Azizi, M. M., Aminzadeh, B., & O'Donnell, J. (2023). A comprehensive review of outdoor thermal comfort in urban areas: Effective parameters and approaches. *Energy and Environment*, *34*(6), 2204–2227. https://doi.org/10.1177/0958305X221116176

Aicha, C., Moussadek, B., & Djamila, D. (2022). The Effect of Sky View Factor on the Thermic Ambiances: Case of Batna City. *International Journal of Innovative Studies in Sociology and Humanities*, *7*(8), 209–220. https://doi.org/10.20431/2456-4931.070820

Albdour, M. S., & Baranyai, B. (2019). Impact of street canyon geometry on outdoor thermal comfort and weather parameters in Pécs. *Pollack Periodica*, *14*(3), 177–187. https://doi.org/10.1556/606.2019.14.3.17

Arif, V., & Yola, L. (2020). The Primacy of Microclimate and Thermal Comfort in a Walkability Study in the Tropics: A Review. *Journal of Strategic and Global Studies*, *3*(1). https://doi.org/10.7454/jsgs.v3i1.1025

Arif, V., & Yola, L. (2022). The Impact of Sky View Factor on Pedestrian Thermal Comfort in Tropical Context: A Case of Jakarta Sidewalk. *Lecture Notes in Civil Engineering*, *161*, 27–33. https://doi.org/10.1007/978-981-16-2329-5_4

Armson, D., Stringer, P., & Ennos, A. R. (2012). The effect of tree shade and grass on surface and globe temperatures in an urban area. *Urban Forestry & Urban Greening*, *11*(3), 245–255. https://doi.org/10.1016/J.UFUG.2012.05.002

Battista, G., de Lieto Vollaro, E., Ocłoń, P., & de Lieto Vollaro, R. (2023). Effects of urban heat island mitigation strategies in an urban square: A numerical modelling and experimental investigation. *Energy and Buildings*, *282*, 112809. https://doi.org/10.1016/J.ENBUILD.2023.112809

Bourbia, F., & Awbi, H. B. (2004). Building cluster and shading in urban canyon for hot dry climate Part 2: Shading simulations. *Renewable Energy*, *29*(2), 291–301. https://doi.org/10.1016/S0960-1481(03)00171-X

Chatzidimitriou, A., & Yannas, S. (2017). Street canyon design and improvement potential for urban open spaces; the influence of canyon aspect ratio and orientation on microclimate and outdoor comfort. *Sustainable Cities and Society*, *33*, 85–101. https://doi.org/10.1016/j.scs.2017.05.019

Chen, L., Ng, E., An, X., Ren, C., Lee, M., Wang, U., & He, Z. (2012). Sky view factor analysis of street canyons and its implications for daytime intra-urban air temperature differentials in high-rise, high-density urban areas of Hong Kong: A GIS-based simulation approach. *International Journal of Climatology*, *32*(1), 121–136. https://doi.org/10.1002/joc.2243

De, B., & Mukherjee, M. (2018). "Optimisation of canyon orientation and aspect ratio in warm-humid climate: Case of Rajarhat Newtown, India." *Urban Climate*, *24*, 887–920. https://doi.org/10.1016/J.UCLIM.2017.11.003

Dunjić, J. (2019). Outdoor Thermal Comfort Research in Urban Areas of Central and Southeast Europe: A Review. *Geographica Pannonica*, *23*(4), 359–373. https://doi.org/10.5937/GP23-24458

Dzyuban, Y., Hondula, D. M., Vanos, J. K., Middel, A., Coseo, P. J., Kuras, E. R., & Redman, C. L. (2022). Evidence of alliesthesia during a neighborhood thermal walk in a hot and dry city. *Science of*

The Total Environment, *834*, 155294. https://doi.org/10.1016/J.SCITOTENV.2022.155294

Elnabawi, M. H., Hamza, N., & Dudek, S. (2013). Use and evaluation of the ENVI-met model for two different urban forms in Cairo, Egypt: Measurements and model simulations. *Proceedings of Building Simulation 2013: 13th Conference of IBPSA*, 13, 2800–2806. https://doi.org/10.26868/25222708.2013.1237

Elrefai, R., & Nikolopoulou, M. (2023). A simplified outdoor shading assessment method (OSAM) to identify outdoor shading requirements over the year within an urban context. *Sustainable Cities and Society*, *97*, 104773. https://doi.org/10.1016/j.scs.2023.104773

Galal, O. M., Sailor, D. J., & Mahmoud, H. (2020). The impact of urban form on outdoor thermal comfort in hot arid environments during daylight hours, case study: New Aswan. *Building and Environment*, *184*, 107222. https://doi.org/10.1016/J.BUILDENV.2020.107222

Glen T. Johnson and Ian Watson. (1984). The determination of view factor in urban canyons. *Americal Metrological Society*. https://www.ptonline.com/articles/how-to-get-better-mfi-results

Harrington, L. J., Frame, D. J., Fischer, E. M., Hawkins, E., Joshi, M., & Jones, C. D. (2016). Poorest countries experience earlier anthropogenic emergence of daily temperature extremes. *Environmental Research Letters*, *11*(5), 055007. https://doi.org/10.1088/1748-9326/11/5/055007

Hess, J., Meister, A., Melnikov, V. R., & Axhausen, K. W. (2023). Geographic Information System-Based Model of Outdoor Thermal Comfort: Case Study for Zurich. *Transportation Research Record*, *2677*(3), 1465–1480. https://doi.org/10.1177/03611981221125211

ICLEI. (2021). *Climate resilient city action plan: Nagpur, Maharashtra, India* (Supported and jointly implemented). http://southasia.iclei.org

IPCC. (2022). *Climate Change 2022: Impacts, Adaptation and Vulnerability*. https://doi.org/ISBN 978-92-9169-161-6

Jamei, E., & Rajagopalan, P. (2017). Urban development and pedestrian thermal comfort in Melbourne. *Solar Energy*, *144*, 681–698. https://doi.org/10.1016/j.solener.2017.01.023

Khaire, J. D., Ortega Madrigal, L., & Serrano Lanzarote, B. (2024). Outdoor thermal comfort in built environment: A review of studies in India. *Energy and Buildings*, *303*, 113758. https://doi.org/10.1016/J.ENBUILD.2023.113758

Kim, Y. J., & Brown, R. D. (2021). A multilevel approach for assessing the effects of microclimatic urban design on pedestrian thermal comfort: The High Line in New York. *Building and Environment*, *205*, 108244. https://doi.org/10.1016/j.buildenv.2021.108244

Konarska, J., Uddling, J., Holmer, B., Lutz, M., Lindberg, F., Pleijel, H., & Thorsson, S. (2016). Transpiration of urban trees and its cooling effect in a high latitude city. *International Journal of Biometeorology*, *60*(1), 159–172. https://doi.org/10.1007/S00484-015-1014-X/FIGURES/8

Kotharkar, R., Bagade, A., & Agrawal, A. (2019). Investigating Local Climate Zones for Outdoor Thermal Comfort Assessment in an Indian City. *Geographica Pannonica*, *23*(4), 318–328. https://doi.org/10.5937/gp23-24251

Kotharkar, R., Dongarsane, P., & Keskar, R. (2023). Determining influence of urban morphology on air temperature and heat index with hourly emphasis. *Building and Environment*, *233*, 110044. https://doi.org/10.1016/j.buildenv.2023.110044

Li, Y., Huang, N., & He, J. (2023). Analytical evaluation of thermal comfort in the pedestrian environment using pedestrian shade space distribution. *Urban Climate*, *51*, 101665. https://doi.org/10.1016/J.UCLIM.2023.101665

Lin, T. P. (2009). Thermal perception, adaptation and attendance in a public square in hot and humid regions. *Building and Environment*, *44*(10), 2017–2026. https://doi.org/10.1016/J.BUILDENV.2009.02.004

Lin, T. P., & Matzarakis, A. (2008). Tourism climate and thermal comfort in Sun Moon Lake, Taiwan. *International Journal of Biometeorology*, *52*(4), 281–290. https://doi.org/10.1007/s00484-007-0122-7

Lin, T. P., Matzarakis, A., & Hwang, R. L. (2010). Shading effect on long-term outdoor thermal comfort. *Building and Environment*, *45*(1), 213–221. https://doi.org/10.1016/j.buildenv.2009.06.002

Lindberg, F., & Grimmond, C. S. B. (2011). The influence of vegetation and building morphology on shadow patterns and mean radiant temperatures in urban areas: Model development and evaluation. *Theoretical and Applied Climatology*, *105*(3), 311–323. https://doi.org/10.1007/S00704-010-0382-8/FIGURES/12

Lobaccaro, G., Acero, J. A., Martinez, G. S., Padro, A., Laburu, T., & Fernandez, G. (2019). Effects of orientations, aspect ratios, pavement materials and vegetation elements on thermal stress inside typical urban canyons. *International Journal of Environmental Research and Public Health, 16*(19), 3574. https://doi.org/10.3390/ijerph16193574

Ma, X., Zhao, J., Zhang, L., Wang, M., & Cheng, Z. (2020). *The Deviation between the Field*

Measurement and ENVI-met Outputs in Winter- A Cases Study in a Traditional Dwelling Settlement of China. https://doi.org/10.21203/RS.3.RS-94479/V1

Manavvi, S., & Milosevic, D. (2025). Chasing cool: Unveiling the influence of green-blue features on outdoor thermal environment in Roorkee (India). *Building and Environment*, *267*, 112238. https://doi.org/10.1016/J.BUILDENV.2024.112238

Marcotullio, P. J., Keßler, C., Quintero Gonzalez, R., & Schmeltz, M. (2021). Urban Growth and Heat in Tropical Climates. *Frontiers in Ecology and Evolution*, *9*, 616626. https://doi.org/10.3389/FEVO.2021.616626/BIBTEX

Matzarakis, A. (2009). Additional features of the RayMan model. *The Seventh International Conference on Urban*, *July*, 3–6. http://www.urbanclimate.net/matzarakis1/papers/ICUC7_rayman_374543-1-090330185705-002.pdf

Matzarakis, A., & Mayer, H. (1996, December). *Another kind of environmental stress: Thermal stress*. WHO Collaborating Centre for Air Quality Management and Air Pollution Control, Institute for Water, Soil and Air Hygiene – Federal Environmental Agency (Newsletter No. 18).

Meshram, D. S. (2011). Institute of Town Planners. *India Journal 8-4*, 1–20.

Middel, A., Selover, N., Hagen, B., & Chhetri, N. (2016). Impact of shade on outdoor thermal comfort—a seasonal field study in Tempe, Arizona. *International Journal of Biometeorology*, *60*(12), 1849. https://doi.org/10.1007/S00484-016-1172-5

Mohite, S., & Surawar, M. (2024a). Assessing Pedestrian Thermal Comfort to Improve Walkability in the Urban Tropical Environment of Nagpur City. *Geographica Pannonica*, *28*(1), 71–84. https://doi.org/10.5937/gp28-48166

Mohite, S., & Surawar, M. (2024b). Assessment and prediction of pedestrian thermal comfort through machine learning modelling in tropical urban climate of Nagpur City. *Theoretical and Applied Climatology*, *2006*, 1–23. https://doi.org/10.1007/s00704-024-04967-x

Mohite, S., & Surawar, M. (2024c). Impact of urban street geometry on outdoor pedestrian thermal comfort during heatwave in Nagpur city. *Sustainable Cities and Society*, *108*(April), 105450. https://doi.org/10.1016/j.scs.2024.105450

Paul, T., Daketi, S., Rao, K. M., & Chundeli, F. A. (2025). A qualitative approach for investigating thermal discomfort in the outdoor environment of a World Heritage Site: A case study of Hampi, India. *Geographica Pannonica, 29*(3), 172–193. https://doi.org/10.5937/gp29-57738

Porwal, S., Mandal, S. K., Banerjee, S., & Abdul, A. P. J. (2025). Factors Influencing Outdoor Thermal Comfort: A Review. *International Research Journal of Multidisciplinary Scope (IRJMS)*, *6*(2), 478–487. https://doi.org/10.47857/irjms.2025.v06i02.03123

Qaid, A., & Ossen, D. R. (2015). Effect of asymmetrical street aspect ratios on microclimates in hot, humid regions. *International Journal of Biometeorology*, *59*(6), 657–677. https://doi.org/10.1007/S00484-014-0878-5/FIGURES/15

Raman, V., Kumar, M., Sharma, A., & Matzarakis, A. (2021). A quantitative assessment of the dependence of outdoor thermal-stresses on tree-building morphology and wind: A case-study in sub-tropical Patna, India. *Sustainable Cities and Society*, *73*, 103085. https://doi.org/10.1016/J.SCS.2021.103085

Ratnayake, C. W., Perera, N. G. R., & Emmanuel, R. (2022a). Street Tree Planting Patterns to Modify the Sky View Factor for Outdoor Thermal Comfort Enhancement. *FARU Journal*, *9*(2), 1–1. https://doi.org/10.4038/FARUJ.V9I2.167

Russo, S., Sillmann, J., Sippel, S., Barcikowska, M. J., Ghisetti, C., Smid, M., & O'Neill, B. (2019). Half a degree and rapid socioeconomic development matter for heatwave risk. *Nature Communications*, *10*(1), 1–9. https://doi.org/10.1038/s41467-018-08070-4

Sayad, B., Alkama, D., Ahmad, H., Baili, J., Aljahdaly, N. H., & Menni, Y. (2021). Nature-based solutions to improve the summer thermal comfort outdoors. *Case Studies in Thermal Engineering*, *28*. https://doi.org/10.1016/J.CSITE.2021.101399

Segura, R., Krayenhoff, E. S., Martilli, A., Badia, A., Estruch, C., Ventura, S., & Villalba, G. (2022). How do street trees affect urban temperatures and radiation exchange? Observations and numerical evaluation in a highly compact city. *Urban Climate*, *46*, 101288. https://doi.org/10.1016/J.UCLIM.2022.101288

Sharmin, T., & Steemers, K. (2013). Effect of Canyon Geometry on Outdoor Thermal Comfort. *PLEA2013 - 29th International Conference Proceedings: Sustainable Architecture for a Renewable Future, Munich, Germany. 10-12 September 2013*, *September*. https://mediatum.ub.tum.de/doc/1169310/file.pdf

Siqi, J., Yuhong, W., & Nyuk Hien, W. (2023). The effect of urban greening on pedestrian's thermal comfort and walking behaviour. *E3S Web of Conferences*, *396*. https://doi.org/10.1051/e3sconf/202339605013

Speak, A., Montagnani, L., Wellstein, C., & Zerbe, S. (2020). The influence of tree traits on urban ground surface shade cooling. *Landscape and Urban*

Planning, *197*, 103748. https://doi.org/10.1016/J.LANDURBPLAN.2020.103748

Srivanit, M., & Jareemit, D., (2019, December 1). Modelling the Urban Microclimate Effects of Street Configurations on Thermal Environment in the Residential Townhouse of Bangkok, Thailand. *1st International Conference on Recent Advances in Science and Technology (ICORAST 2019), MalaysiaAt: Kuala Lumpur, Malaysia*. https://doi.org/10.13140/RG.2.2.17499.21283

Surawar, Meenal; Kotharkar, R. (2017). Assessment of Urban Heat Island through Remote Sensing in Nagpur Urban Area Using Landsat 7 ETM+ satellite images. *International Journal of Urban and Civil Enginering*, *11*(7), 868–874. https://doi.org/10.5281/ZENODO.1131073

Tumini, I., Higueras García, E., & Baereswyl Rada, S. (2016). Urban microclimate and thermal comfort modelling: strategies for urban renovation. *International Journal of Sustainable Building Technology and Urban Development*, *7*(1), 22–37. https://doi.org/10.1080/2093761X.2016.1152204

Vailshery, L. S., Jaganmohan, M., & Nagendra, H. (2013). Effect of street trees on microclimate and air pollution in a tropical city. *Urban Forestry & Urban Greening*, *12*(3), 408–415. https://doi.org/10.1016/J.UFUG.2013.03.002

Vasilikou, C., & Nikolopoulou, M. (2020). Outdoor thermal comfort for pedestrians in movement: thermal walks in complex urban morphology. *International Journal of Biometeorology*, *64*(2), 277–291. https://doi.org/10.1007/s00484-019-01782-2

Watanabe, S., & Ishii, J. (2016). Effect of outdoor thermal environment on pedestrians' behavior selecting a shaded area in a humid subtropical region. *Building and Environment*, *95*, 32–41. https://doi.org/10.1016/j.buildenv.2015.09.015

Willmott, C. J. (1982). Some comments on the evaluation of model performance. *Bulletin - American Meteorological Society*, *63*(11), 1309–1313. https://doi.org/10.1175/1520-0477(1982)063<1309:SCOTEO>2.0.CO;2

Xu, L., Gopalakrishnan, S., & Schroepfer, T. (2023). *Assessment of overhead environments on pedestrian thermal comfort in a dense urban district*. https://doi.org/10.1051/e3sconf/202339605012

Yilmaz, S., Kurt, A., & Gölcü, M. (2023). ENVI-met Simulations of the Effect of Different Landscape Design Scenarios on Pedestrian Thermal Comfort: Haydar Aliyev Street. *Yuzuncu Yil University Journal of Agricultural Sciences*, *33*(3), 338–353. https://doi.org/10.29133/yyutbd.1265752

Zhang, M., You, W., Qin, Q., Peng, D., Hu, Y., Gao, Z., & Buccolieri, R. (2022). Investigation of typical residential block typologies and their impact on pedestrian-level microclimate in summers in Nanjing, China. *Frontiers of Architectural Research*, *11*(2), 278–296. https://doi.org/10.1016/J.FOAR.2021.10.008

Zhang, Y., Du, X., & Shi, Y. (2017). Effects of street canyon design on pedestrian thermal comfort in the hot-humid area of China. *International Journal of Biometeorology*, *61*(8), 1421–1432. https://doi.org/10.1007/S00484-017-1320-6

Zhao, H., Zhao, L., Zhai, Y., Jin, L., Meng, Q., Yan, J., Wu, R., & Brown, R. D. (2024). The impact of dynamic thermal experiences on pedestrian thermal comfort: A whole-trip perspective from laboratory studies. *Building and Environment*, *258*, 111599. https://doi.org/10.1016/J.BUILDENV.2024.111599